

Physics-based Uncertainty Quantification for Megathrust Earthquake Potential Using Reduced-Order Modeling

Gabrielle Hobson (ghobson@ucsd.edu) and Dave A. May
Institute of Geophysics and Planetary Physics, University of California San Diego

AGU23 T41D-0247



MTMOD: Megathrust Modeling Framework
NSF-EAR 2121568
sites.utexas.edu/mtmod/

Motivation

Megathrust earthquakes are the largest on Earth, capable of causing strong ground shaking and generating tsunamis. Rupture limits are thought to be primarily temperature-controlled^[1,2], but thermal models used to predict the potential locations of the rupture limits^[3,4] are naturally subject to uncertainty^[5].

- How sensitive is the estimated seismogenic zone extent to variation in model input parameters?
- How uncertain are estimates of the seismogenic zone extent, given uncertainty in model input parameters?

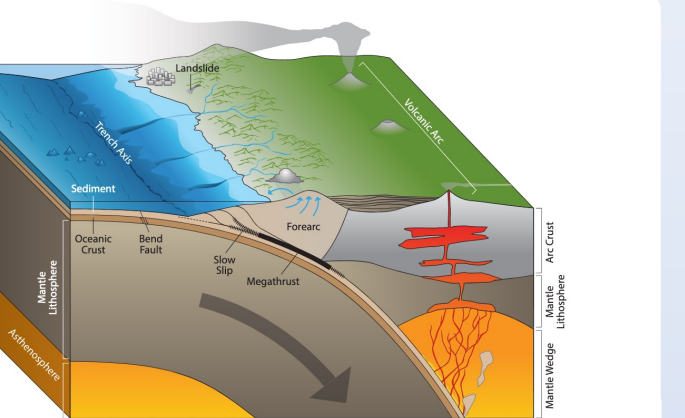


Fig 1. Modified from Fig 1.4 of [6].

Methods

Subduction Zone Thermal Model

We simulate the 2D thermal structure of a regional subduction zone by solving the coupled, nonlinear conservation of mass, conservation of momentum, and steady-state advection-diffusion equations:

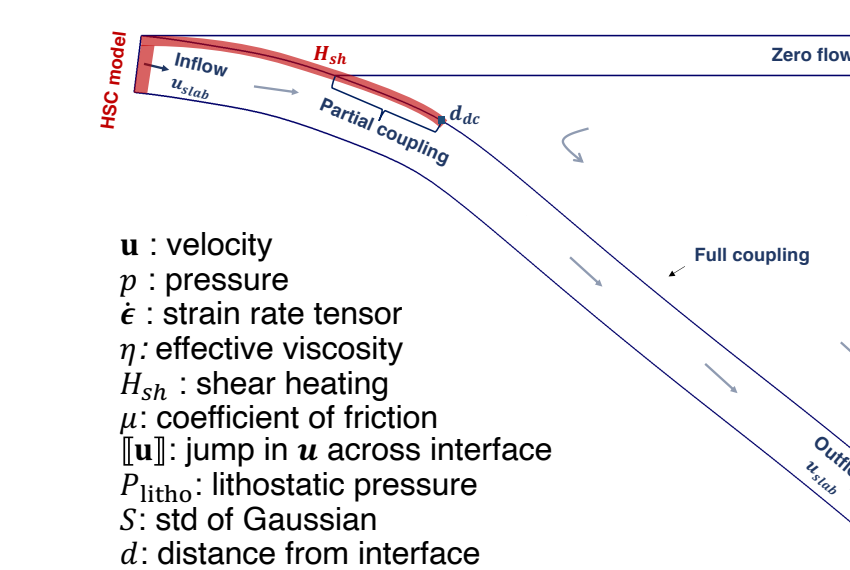
$$\nabla \cdot (\mathbf{u} \dot{\epsilon}) - \nabla p = 0,$$

$$\rho c_p(\mathbf{u} \cdot \nabla)T = \nabla \cdot (k \nabla T) + H_{sh}.$$

This approach closely follows the literature [e.g. 7, 8, 9, 10]. The mantle wedge viscosity $\eta(T, \mathbf{u})$ captures the diffusion and dislocation creep mechanisms. The shear heating source term is modeled using a Gaussian centered on the slab interface:

$$H_{sh} = \frac{\mu \|\mathbf{u}\| P_{litho}}{S \sqrt{2\pi}} \exp\left(-\frac{d^2}{2S^2}\right).$$

We solve the equations in weak form via the Finite Element Method using FEniCS 2019.1.0 [11] and verify against [10].



Reduced-Order Modeling

We build low-dimensional surrogate models (ROMs) that capture the characteristic behavior of the full-order thermal model (the FOM) but are much faster to evaluate. The interpolated Proper Orthogonal Decomposition (iPOD) [12, 13, 14, 15] is:

- Data-driven: gives the optimal basis for a dataset of forward model solutions, and therefore is amenable to nonlinear problems.
- Non-intrusive: does not require altering the forward model code, takes only FOM output as data.

The iPOD process:

- Assemble FOM solutions, i.e. temperature fields \hat{T}_i , into columns of the data matrix \mathbf{X} , which has a corresponding parameter vector \mathbf{Q} .

$$\mathbf{X}_{M \times N} = \begin{bmatrix} \hat{T}_1 & \hat{T}_2 & \hat{T}_3 & \dots & \hat{T}_N \end{bmatrix} = \begin{bmatrix} \hat{T}_1 & \hat{T}_2 & \hat{T}_3 & \dots & \hat{T}_N \end{bmatrix}$$

$$\mathbf{Q} = [\mathbf{q}_1, \mathbf{q}_2, \mathbf{q}_3, \dots, \mathbf{q}_N].$$

- Take the Singular Value Decomposition (SVD): $\mathbf{X} = \mathbf{U} \Sigma \mathbf{V}^T$.

- Interpolate the POD coefficients $\alpha = \Sigma \mathbf{V}^T$ at a new parameter vector $\hat{\mathbf{q}} \notin \mathbf{Q}$ using Radial Basis Function (RBF) interpolation^[16].

- Approximate $\hat{T}(\hat{\mathbf{q}})$ using the interpolated POD coefficients $\hat{\alpha}(\hat{\mathbf{q}})$ and the optimal orthogonal basis \mathbf{U} :

$$\hat{T}(\hat{\mathbf{q}}) = \mathbf{U} \hat{\alpha}.$$

The resulting ROMs can be evaluated 10^4 times faster than the FOM and are accurate to within $< 10\%$, such that D varies by < 1 km. This makes it possible to evaluate the ROM $\mathcal{O}(10^5)$ or $\mathcal{O}(10^6)$ times as required by global sensitivity analysis and uncertainty quantification methods.

Parameter Screening

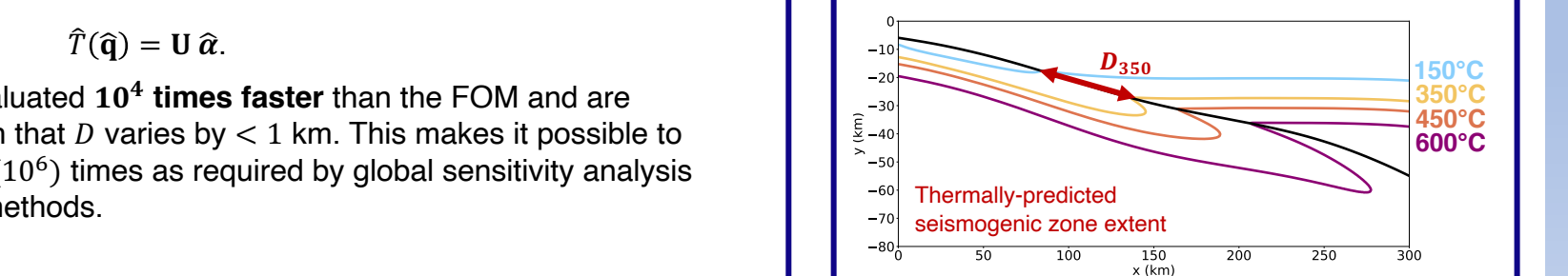
We use global sensitivity analysis via the Method of Morris to determine which parameters have little effect on the quantity of interest - in this case the extent of the seismogenic zone – and can therefore be screened out^[17, 18, 19].

Uncertainty Quantification

To quantify the relationships between input parameters and the estimated seismogenic zone extent, we examine scatterplots and perform simple curvilinear regression analysis. We present scatterplots and R^2 values, where R^2 values close to 1 indicate the polynomial fit is a good estimator of the data.

Quantities of Interest

D : along-slab distance between isotherms representing extent of the seismogenic zone.
 D_{350} : distance from 150°C to 350°C isotherm
 D_{450} : distance from 150°C to 450°C isotherm
 D_{600} : distance from 150°C to 600°C isotherm



Results

I. Sensitivity Analysis

Table 1. Parameter screening results, with important parameters in green and screened parameters in grey. Lists are for Cascadia, Nankai, and Hikurangi.

u_{slab}	Plate convergence rate	cm/yr	[3.0, 5.0], [3.0, 5.0], [3.0, 4.0]
μ	Effective coefficient of friction	~	[0.0, 0.1]
d_{dc}	Depth of decoupling	km	[70, 80]
deg_{pc}	Degree of partial coupling	~	[0.0, 0.1]
T_b	Mantle inflow temperature	K	[1550, 1750]
t_{slab}	Age of incoming lithosphere	Myr	[8, 10], [15, 26], [90, 110]
z_{bc}	Depth of continental geotherm	km	[10, 60]
A_{diff}	Diff. creep pre-exp. factor	Pa s	[1.2×10^9 , 2.4×10^{10}]
E_{diff}	Diff. creep activation energy	J/mol	[300×10^3 , 450×10^3]
A_{dist}	Disloc. creep pre-exp. factor	Pa s ^(1/n)	[1×10^4 , 5×10^4]
E_{dist}	Disloc. creep activation energy	J/mol	[480×10^3 , 560×10^3]
n	Power law exponent	~	[0, 3.5]

- We build ROMs using temperature fields from forward models run for nine profiles of Cascadia, Nankai, and Hikurangi.
- Global sensitivity analysis reveals that the extent of the seismogenic zone is sensitive to variation in parameters related to slab motion, coupling, and the thermal structure of the incoming lithosphere.
- Parameters in the mantle wedge rheological flow law and far-field boundary condition can be screened out.

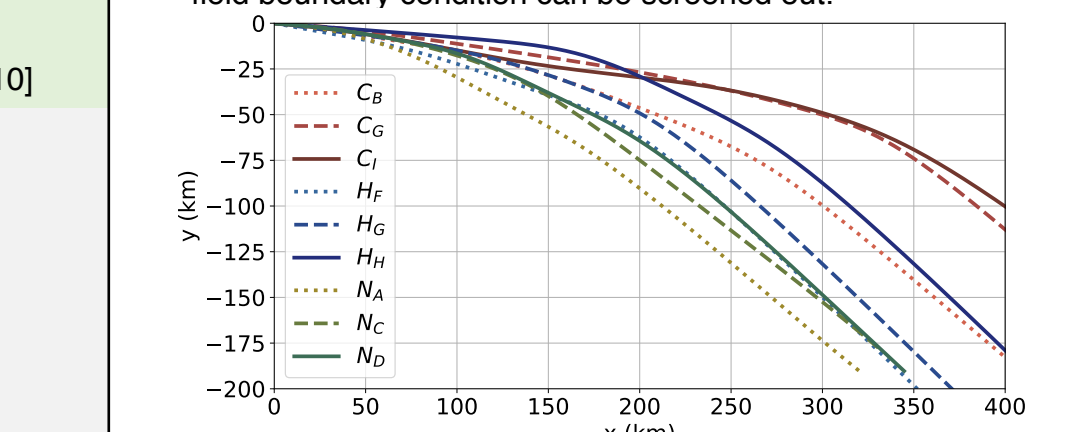


Fig 2. The range of slab interface profiles for Cascadia, Hikurangi and Nankai, from Slab 2.0 data [20].

II. Relationship Between Key Parameters and Estimated Seismogenic Zone Extent

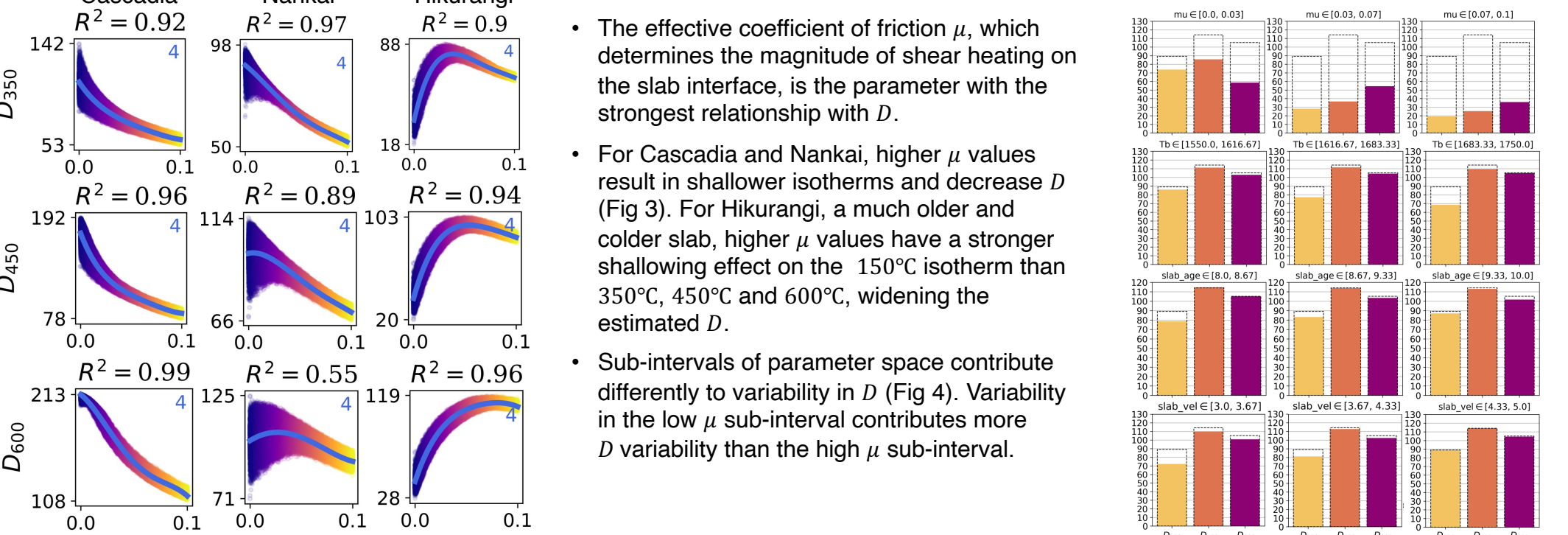


Fig 3. Scatterplots with 10^5 samples in parameter space showing the strong relationship between μ and seismogenic zone extent. Blue lines show the 4th order polynomial regression, with R^2 reported above.

III. Uncertainty in Estimated Seismogenic Zone Extent

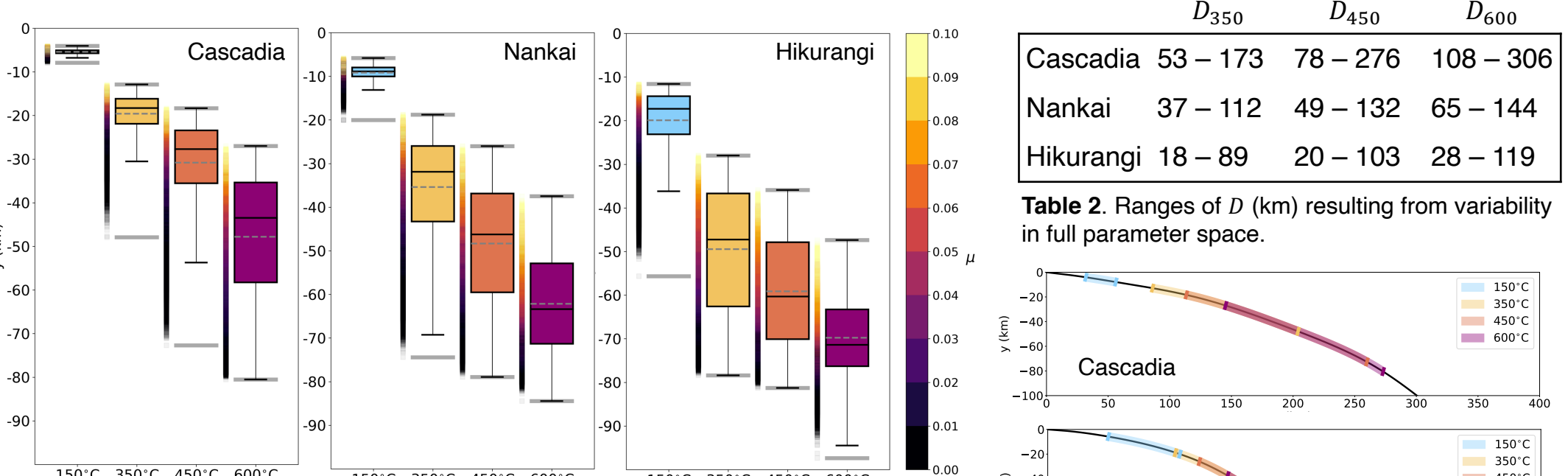


Fig 4. Cascadia D variability (km) when samples are taken in sub-intervals of parameter space. Dotted lines show variability from full parameter space.

Comparison to Maximum Depth of Thrust Faulting

We examine a selection of uncertainty ranges for μ from the literature and compare isotherm intersection depths to the max depth of thrust faulting, z_T , from [21].

- Published uncertainty ranges result in large variability in the estimated isotherm intersection depths.
- Cascadia: both the 350°C and 450°C isotherm IQRs overlap the estimated range of z_T .
- Nankai: the model-predicted 350°C isotherm depths overlap the z_T depth range, but the IQRs are deeper than the z_T depth range.
- Hikurangi: higher values of μ result in 350°C isotherm depths for Hikurangi that overlap z_T for the S margin, but are significantly deeper than z_T for the N margin. This agrees with studies [23, 24] arguing that along-strike variance in locking depth cannot be solely thermally controlled.

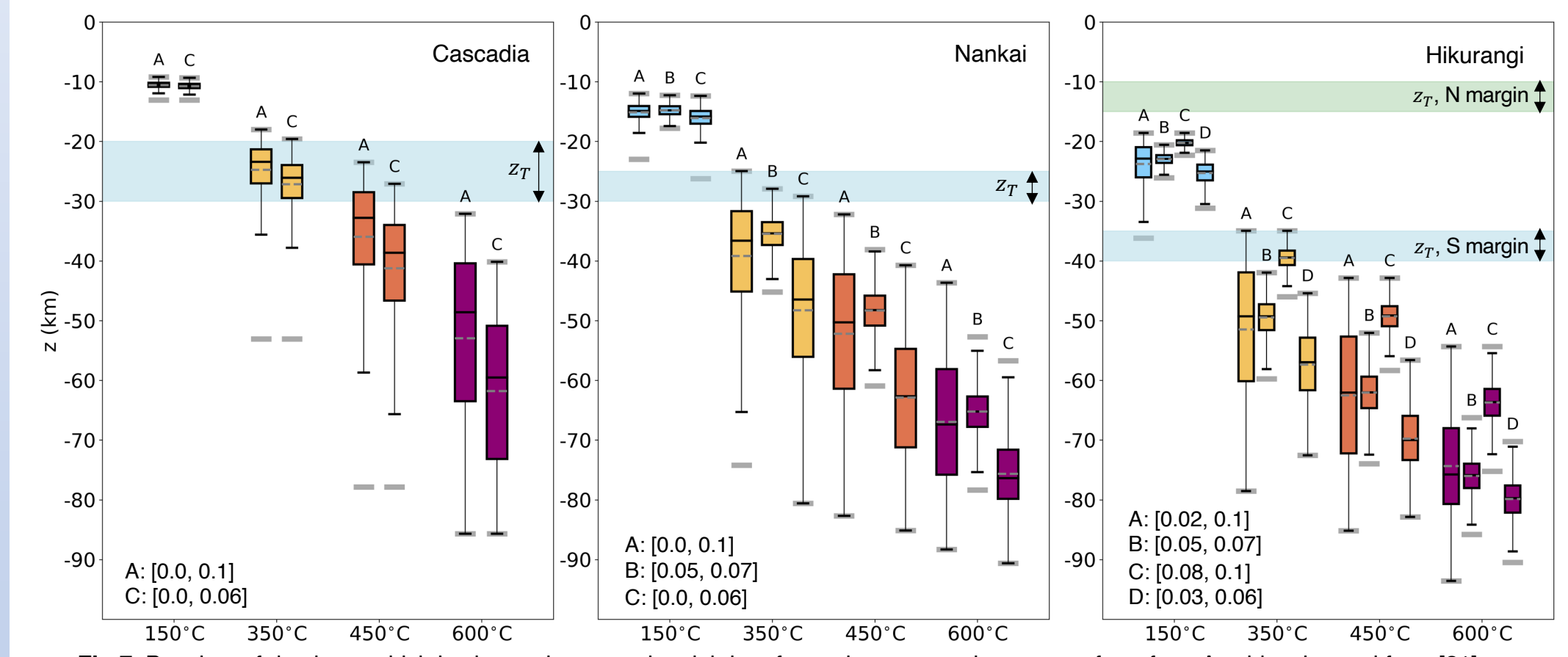


Fig 7. Boxplots of depths at which isotherms intersect the slab interface, given uncertainty ranges for μ from [21]. B: preferred interval from [21], C: interval from [25], D: range inferred by [21] from [23]. We limit uncertainty ranges to [0, 0.1] where they exceed 0.1. Note that for Cascadia, z_T must be estimated from the line of 20% locking^[21, 22] due to a lack of focal mechanisms.

Key Findings

Estimated seismogenic zone extent D is sensitive to variability in effective coefficient of friction μ .

- Variability in the low range of μ values contributes most of the variability in D estimates.

Uncertainty in key parameters results in significant uncertainty in estimated M_w (Table 3).

- We use an empirical scaling relationship for large and great earthquakes from [26] who observe that moment scales with $A^{3/2}$, where A is the effective rupture area. We conservatively assume $A = D^2$ as in [21] and compute $M_w = \frac{2}{3}(\log_{10}(M_0) - 9.1)$ to obtain our estimates^[27].

Considering uncertainty in the choice of downdip limit isotherm results in higher estimated D and M_w .

- Lab experiments on olivine friction indicates the transition from velocity weakening to velocity strengthening occurs at $\sim 600^\circ\text{C}$ [28], which results in significantly higher estimates of D and M_w (Table 3).



github.com/gabriellemhobson/SZ_2D_thermal_structure

	350°C	450°C	600°C
Cascadia	7.6 – 8.6	7.9 – 9.0	8.2 – 9.1
Nankai	7.3 – 8.2	7.5 – 8.4	7.8 – 8.5
Hikurangi	6.6 – 8.0	6.7 – 8.2	7.0 – 8.3

Table 3. Ranges of M_w given uncertainty in D , for each choice of downdip limit isotherm.

References

- [1] Hyndman and Wang (1993). *J. Geophys. Res. Solid Earth*, 98 (B2), 2039–2060.
- [2] Tichelar and Ruff (1993). *J. Geophys. Res. Solid Earth*, 98 (B2), 2017–2037.
- [3] Smith et al. (2013). *GRL*, 40 (8), 1528–1533.
- [4] Kroll et al. (2013). *Geophys. J. Int.*, 193 (3), 1530–1540.
- [5] Peacock (2013). *Geosphere*, 16 (4): 933–952.
- [6] McGuire, Plank, et al. (2013). *Computers & Fluids*, 36 (3), 499–512.
- [7] Walton et al. (2013). *Applied Mathematical Modelling*, 37, 8930–8945.
- [8] Currie et al. (2004). *EPSL*, 223 (1), 35–48.
- [9] Wada et al. (2008). *J. Geophys. Res. Solid Earth*, 113 (B4).
- [10] van Keeken et al. (2008). *PEPI*, 171 (1), 187–197.
- [11] Logg et al. (2012). *Springer, Berlin, Heidelberg*.
- [12] Holmes et al. (2012). *Cambridge University Press, Cambridge*.
- [13] Ly & Tran (2001). *Mathematical and Computer Modelling*, 33 (1), 223–236.
- [14] Boettcher et al. (2007). *Geophys. J. Int.*, 171 (3), 1213–1222.
- [15] McCaffrey et al. (2008). *Nature Geosci.*, 1, 316–320.
- [16] Gao and Wang (2014). *Science*, 345 (6200), 1038–1041.
- [17] Hayes et al. (2018). *Science*, 362.
- [18] England (2018). *J. Geophys. Res. Solid Earth*, 123, 7165–7202.
- [19] Schmalzle et al. (2014). *Geochim. Geophys. Geosyst.*, 15, 1515–1532.
- [20] McCaffrey et al. (2008). *Nature Geosci.*, 1, 316–320.
- [21] Holme et al. (2012). *Cambridge University Press, Cambridge*.
- [22] Schmalzle